# Composing Power Flow Patterns through Coordinated Dispatch of Energy Packets


1st Dominik Schulz
*Institute of Electrical Engineering (ETI)*
*Karlsruhe Institute of Technology (KIT)*
Karlsruhe, Germany
dominik.schulz@kit.edu

2nd Klemens Schneider
*Institute of Telematics (TM)*
*Karlsruhe Institute of Technology (KIT)*
Karlsruhe, Germany
klemens.schneider@kit.edu

3rd Marcel Weßbecher
*Institute for Automation and Applied Informatics (IAI)*
*Karlsruhe Institute of Technology (KIT)*
Karlsruhe, Germany
marcel.wessbecher@kit.edu

4th Veit Hagenmeyer
*Institute for Automation and Applied Informatics (IAI)*
*Karlsruhe Institute of Technology (KIT)*
Karlsruhe, Germany
veit.hagenmeyer@kit.edu

5th Martina Zitterbart
*Institute of Telematics (TM)*
*Karlsruhe Institute of Technology (KIT)*
Karlsruhe, Germany
martina.zitterbart@kit.edu

6th Marc Hiller
*Institute of Electrical Engineering (ETI)*
*Karlsruhe Institute of Technology (KIT)*
Karlsruhe, Germany
marc.hiller@kit.edu



***Abstract*—The increasing share of distributed renewable generation and electrification poses challenges to the existing power grid and its operation. To address these challenges, the concept of an Energy Packet Grid (EP Grid) has been proposed that uses selected internet design principles for power grids. This paper builds upon the EP Grid architecture and explores the shaping of power flows through a coordinated dispatch of energy packets. It introduces parallel energy packet transfers to maintain constant power over specific durations and to improve the approximation of continuous load or supply curves. A scenario manager is integrated into the architecture to coordinate specified sequences of energy packet transfers. Measurements demonstrate two scenarios of possible energy packet sequences.**



***Index Terms*—energy packets, energy packet grid, energy internet, power flow control, power electronic grid, microgrid**


## I. Introduction

The transition toward a decarbonized power system, characterized by distributed renewable generation and growing electrification of heat and transport sectors, presents challenges to the conventional power grid and its operational framework. Deployed power lines and grid equipment were not designed to support the power flows arising from this structural change [1], [2]. Additionally, the volatile nature of renewable sources implies a shift from the control of the power supply to increasingly necessary flexibility on the demand side [3]. Microgrids and related concepts [4], [5] address these challenges by local and autonomous control of connected participants, with the possibility to operate in an islanded mode. While these approaches reduce the control complexity in the future grid, they lack a clear solution to coordinate the allocation of shared operating equipment such as power lines and transformers. In recent years, the concept of an Energy Internet, which applies selected design principles of the Internet to power grids, has gained renewed interest [6]–[12]. In [13]–[15], the authors propose a packetized energy management inspired by communication theory concepts applied to thermostats and electric vehicle (EV) charging schemes. A more extensive approach called the Energy Packet Grid (EP Grid) was presented in [16] and [17], where in its final stage the majority of power flows in the grid are composed of energy packets with discrete power and duration. This approach allows to maintain the local power balance through pre-arranged power flows, while also respecting the limits of the grid equipment and the precise routing of power flows.

This paper further develops the envisioned architecture introduced in [16] by detailing the possibility to shape power flows in the EP Grid through a coordinated dispatch of energy packets. These power flows can be designed to maintain a constant power over specific durations, despite variations in their composition from different packets. In addition, parallel energy packet (EP) transfers from one or multiple devices are introduced and implemented to improve the approximation of desired continuous load or supply curves. To demonstrate these capabilities, a scenario manager is integrated into the architecture to coordinate specified sequences of EP transfers.

## II. Power Flows in the EP Grid

The proposed EP Grid [16] is based on two main concepts: energy packets and the cell concept. Energy packets represent discrete units with predefined power shapes, enabling actors in the EP Grid to organize energy transports efficiently. This packet-based operation leverages the multiplexing gain to optimize resource utilization while respecting operational limits and facilitating the scheduling of future power flows, as well as energy management. Inspired by the idea of the internet of creating a network of networks, the power grid is divided into smaller sub-networks known as EP cells. These self-organized EP cells can be configured to operate with DC or asynchronous AC voltage, independent of adjacent EP cells. This design


This work was supported by the KIT Future Fields Stage 2 funding program

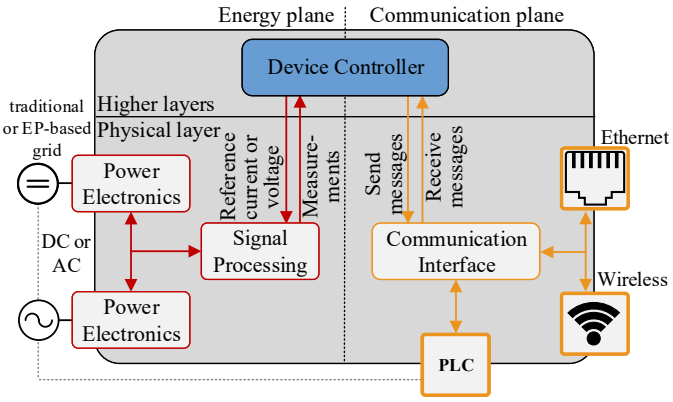


Fig. 1: Architecture of an EP device based on [16]

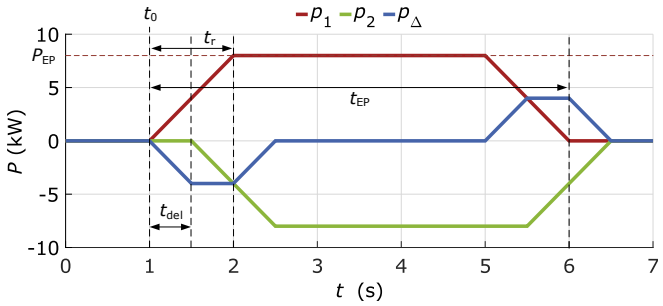


Fig. 2: Power curves for an EP transfer with communication latency

principle offers the advantages of a more decoupled grid and enables the integration of existing infrastructure.

Participants of an EP cell, called EP devices, collaboratively manage currents and the power balance in the EP cell, with at least one device responsible for maintaining the EP cell voltage. The architecture of an EP device is depicted in Fig. 1. Each EP device is equipped with communication interfaces and power electronics, that allow it to assume the role of a voltage or current controller in its EP cell. The communication architecture between EP devices can be realized using multiple technologies.

The communication plane is used to agree upon an EP transfer between two participants, together with its required parameters. For a trapezoidal power curve, these are the total packet energy $W_{\mathrm{EP}}$, ramping time $t_{\mathrm{r}}$, and the stationary power level $P_{\mathrm{EP}}$. The total energy exchanged is defined by the time integral of the power curve $W_{\mathrm{EP}} = \int_{t_0}^{t_0+t_{\mathrm{EP}}} p_{\mathrm{EP}}(\tau)d\tau$ where $t_{\mathrm{EP}}$ is the total packet duration including ramping phases. Fig. 2 shows power curves for an example EP transfer. In this example, a communication latency of $t_{\mathrm{del}}$ is included. In order to satisfy the power equilibrium $\sum_i p_i = 0$ in the EP cell, the negative sum of the two power curves $p_\Delta = -(p_1 + p_2)$ needs to be supplied by another EP device, e.g. the EP cell voltage controller.

A key aspect of the EP-based operation is the necessity of

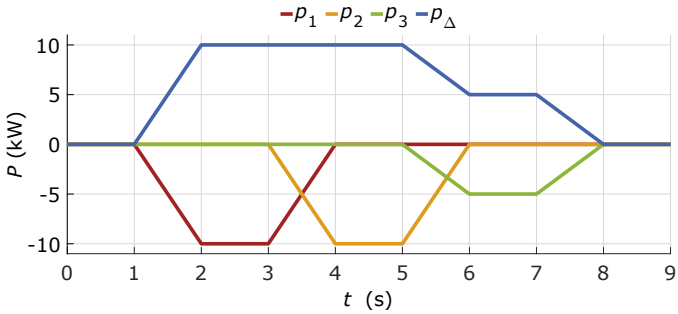


Fig. 3: Power curves for chained packet sequences

energy storage in the EP devices if they act as an interface for loads or sources with continuous power flows. While the continuous character of some electrical appliances can be controlled to act in a discrete manner, e.g. heat pumps or water heaters that turn on and off as required, this is not possible in all cases. The energy storage has to provide the power and energy mismatch between the discrete energy packet power levels $p_{\mathrm{EP}}$ and the connected continuous power demand $p_{\mathrm{cont}}$:

$$W_{\mathrm{storage}} = \int_{t_0}^{t_0+t_{seq}} \left[\sum_i p_{\mathrm{EP,i}}(\tau) - p_{\mathrm{cont}}(\tau)\right] d\tau \quad (1)$$

with

$$t_{\mathrm{seq}} = \sum_i t_{\mathrm{EP,i}}\,. \quad (2)$$

This mismatch can be reduced with two mechanisms. First, by allowing multiple packet transfers in parallel, a continuous power curve can be better approximated by requesting additional packets as required. The second mechanism consists of consecutive packet transfers arranged in a chained sequence with overlapping ramping phases, in order to achieve a continuous power flow for an EP device. Both concepts are shown in Fig. 3. A second sequence with short ramping phases is shown in Fig. 4. This sequence highlights the ability of an EP device to engage in simultaneous EP transfers with multiple other EP devices and thus to shape its total power exchange as required. Also visible is the option to initially negotiate a longer transfer for the base demand and subsequently request additional packets if necessary. By employing parallel EP transfers, it becomes possible to reduce the power and duration of planned EP transfers, aligning them more accurately with the continuous demand or supply connected to the device. These abilities are achieved while preserving the benefits of observing equipment limits, possible multiplexing gains, and power flow routing capabilities.

## III. Implementation of Coordinated Energy Packet Transfers

The coordinated transfers of energy packets are implemented using three defined interfaces in the communication plane. First, two participants within an EP cell need to agree upon a subsequent energy transfer. Second, for the central coordination of multiple transfers used in this paper, a managing instance is integrated as a higher control layer that can

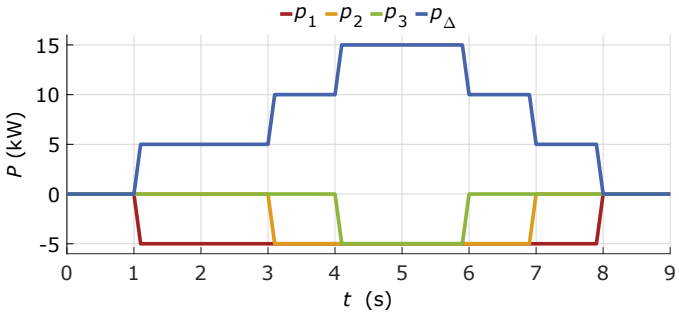


Fig. 4: Power curves for concurrent packet transfers

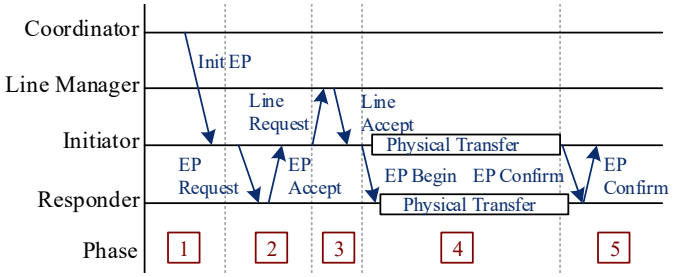


Fig. 5: Message sequence for a single EP transfer

instruct each EP device to start a transfer. Finally, within each EP device, the negotiated transfer parameters have to be passed to the power electronics to physically perform the EP transfer in the energy plane.

The inter-device communication is achieved using the already developed Simple Energy Packet Transfer (SEPT) protocol [16]. It allows participants within the same EP cell to transfer energy packets to each other according to present and projected power supply and demand. An additional software component termed Line Manager is introduced to ensure that parallel EP transfers do not exceed power line limits. The SEPT messaging sequence is shown in Fig. 5. The two participants of an EP transfer are called the initiator and responder and the initiator can either be absorbing or providing power. The EP transfer starts after a command from the central coordinator in phase (1) and consists of four subsequent phases: (2) energy reservation phase, (3) line capacity reservation phase, (4) energy transfer phase, and (5)

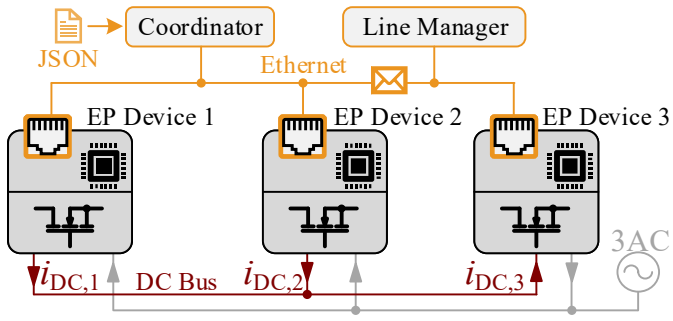


Fig. 6: EP cell network and electrical topology

confirmation phase. During phase 2, the initiator and responder agree upon an EP shape with the parameters described in section II. Upon the approval of the Line Manager in phase 3, the energy packet is transferred in phase 4. The SEPT protocol is implemented in a client application running on the PC of each EP device. This client sends and receives the SEPT messages over TCP. It is able to manage multiple transfers in parallel and communicates the resulting summed power setpoint $p_{\mathrm{set}}(t) = \sum_i p_{\mathrm{EP,i}}(t)$ to the power electronics.

In this work, a central coordinator is responsible for instructing EP devices within the EP cell to start EP transfers. In the envisioned EP grid, individual participants would autonomously determine when to initiate a transfer. This decision could be based on energy storage levels, present and future power supply and demand or other signals such as a dynamic electricity price, but this is outside the scope of this paper. In order to emulate possible packet sequences resulting from this operation in a predictable manner, the EP devices are configured to receive the initiation message from the central coordinator instead. This message includes the intended peer for the transfer, as well as the transfer parameters the device communicates with its peer. This allows to construct a predefined sequence of EP transfers in the cell that results in the desired power flows. The scenario schedule is stored as a JSON configuration file, where each EP transfer has an associated starting time.b The central coordinator follows this schedule to send the initialization messages to the SEPT clients in phase 1 of Fig. 5 as soon as the specified time is reached. Note that Fig. 5 only shows the sequence of messages resulting from one initialization message. During a scenario, the coordinator may initiate multiple transfers on the same device in parallel.

To ensure effective communication between the SEPT client and the low-level control of the power electronics within each device, a dedicated protocol was developed. This protocol enables the exchange of power setpoints and measurement values with a FreeRTOS real-time operating system running on the signal processing platform responsible for controlling the power electronics over an Ethernet connection.

Two modes of energy packets are possible when determining the setpoints for the low-level control. In the first mode, the voltage within the EP cell is assumed to be constant at its operating value $v_{\mathrm{op}}$. The required current for a negotiated power level $p_{\mathrm{EP}}$ can then be calculated as $i^*_{\mathrm{EP}} = \frac{p_{\mathrm{EP}}}{v_{\mathrm{op}}}$. As a disadvantage, the energy content of the transferred packet would differ from the negotiated amount in case the voltage in the EP cell varies. Therefore, the second mode calculates the current setpoints based on the instantaneous measured voltage in the EP cell. This results in predictable amounts of transferred energy but complicates the task of the Line Manager as the resulting currents $i_{\mathrm{EP}}$ are unknown in this mode. A detailed comparison as well as a proposed mixed-mode is presented in [18].

Finally, the determined setpoints are tracked by a PI controller with additional feed-forward paths that drives a Dual Active Bridge (DAB) as power stage as explained in Sec. IV.

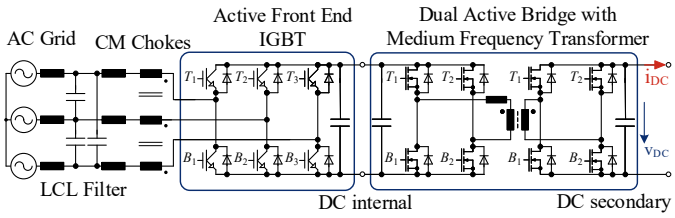


Fig. 7: Hardware topology of the EP devices

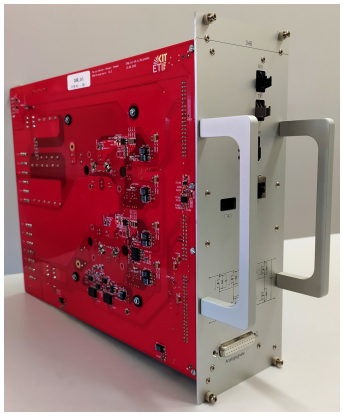

Fig. 8: Dual Active Bridge

One possible network topology and electrical interconnection of an EP cell is shown in Fig. 6.

## IV. Hardware and Low-Level Control of an Energy Packet Device

This section presents the hardware realization of an EP device as defined in section II that is used for the measurements. Additionally, the low-level control for the power electronic modules is described. The hardware realization is discussed in detail in [17]. Each EP device contains a computer and a signal processing platform. This platform is a System-on-Chip based on a Xilinx Zynq™-7030 that consists of two ARM cores and an FPGA. One core runs a FreeRTOS instance that handles the network connectivity, while the second core runs the controls, the global state machine and error handling. The FPGA interfaces the power electronic modules and further periphery. The first module shown in Fig. 7 is a two-level IGBT converter used to control a constant internal DC voltage $v_{\mathrm{DC,int}}$. The second module is a Dual Active Bridge shown in Fig. 8, connected to the internal DC link. It provides galvanic isolation and can control either the secondary DC voltage $v_{\mathrm{DC}}$ or current $i_{\mathrm{DC}}$. The complete realized EP device is depicted in Fig. 9.

The control structure of the AC/DC Active Front End, described in detail in [17], is given in Fig. 10. It assumes an existing AC grid that can be used to arbitrarily inject or withdraw power. The main control objective is the regulation of the internal DC link voltage $v_{\mathrm{DC,int}}$, which is performed by a PI controller in the rotating dq-reference frame. The required currents are transformed into the stationary $\alpha\beta$-coordinate system using a synchronous reference frame phase-locked loop

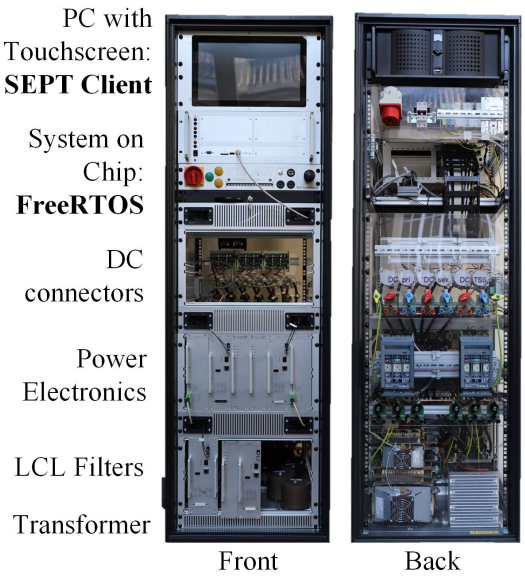


Fig. 9: Complete EP device

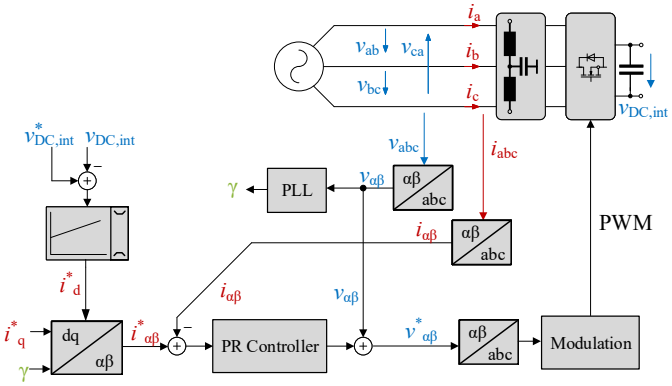


Fig. 10: Control structure of the AC/DC converter with DC link voltage control when connected to an existing AC grid

(SRF-PLL) and then controlled by dampened proportional-resonant (PR) controllers.

The control of the Dual Active Bridge operating in the current-control mode is based on the control approach described in [19]. Its structure is depicted in Fig. 11. Since the subordinate angle calculation already provides accurate open-loop control, the main part of the setpoint $i^*_{\mathrm{DC}}$ is fed forward. An integral controller is added to mitigate remaining control deviations. In order to compensate for the computation, modulation and measurement delay, the input for this controller is delayed by the same amount of time. The sum of the feedforward signal and controller output is passed to a limiter that determines the maximum allowable requested current depending on primary and secondary side voltages $v_{\mathrm{DC,int}}$ and $v_{\mathrm{DC}}$.

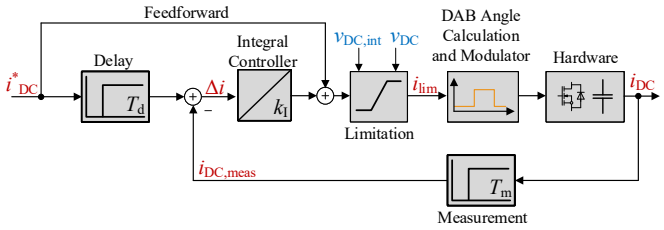


Fig. 11: Control structure of the Dual Active Bridge when operating in current-control mode based on [19]

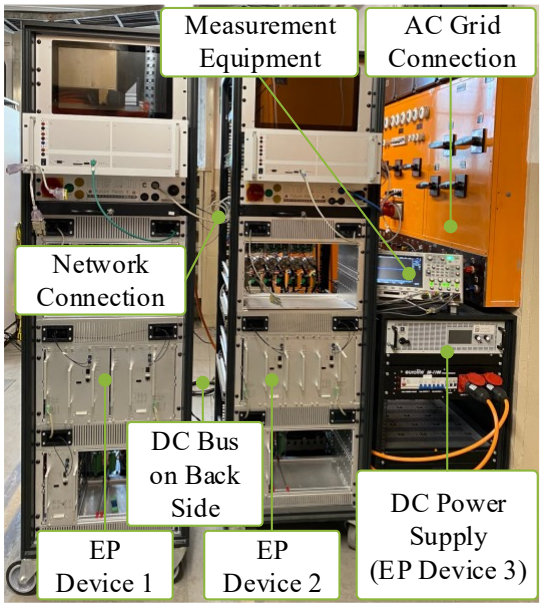


Fig. 12: Laboratory setup as described in Fig. 6

## V. Measurements of Energy Packet Sequences

For the measurements, the network and electrical configuration given in Fig. 6 is used. The laboratory setup is shown in Fig. 12. Two of the EP devices are realized as described in section IV, while the third is replaced by a DC power supply providing a constant DC voltage of $v_{\mathrm{DC}} = 600\,\mathrm{V}$. Each EP device runs a SEPT client. Both the Line Manager and the central coordinator run as separate applications on EP device 1. Since no setpoints need to be transferred to the power supply, its associated SEPT client can run on one of the other computers. When it participates in an EP transfer, it will provide the required current in order to maintain the DC voltage. All messages are exchanged over the local laboratory network. The Line Manager and the SEPT clients are configured to accept all requested transfers so that the scenario schedule is executed as planned.

The AC/DC converter in each device is connected to a common three-phase AC grid shown in gray in Fig. 6. The connected DAB is configured to control its current $i_{\mathrm{DC,x}}$ into the DC EP cell. Through the AC connection, the EP devices can exchange power with the EP cell. This allows arbitrary power curves within the operational limits.

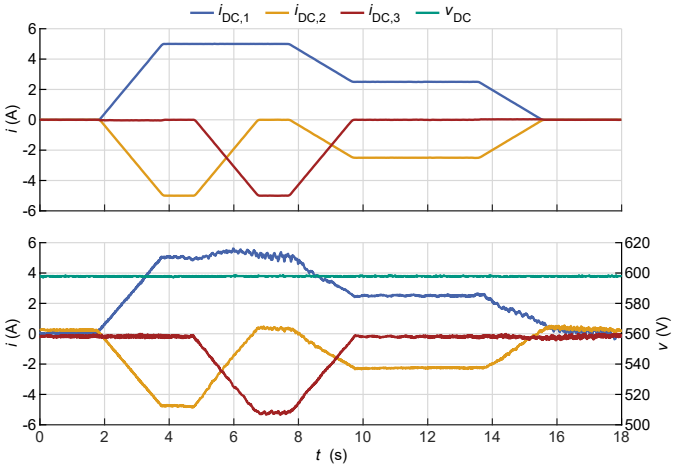


Fig. 13: Measurements for chained EP transfer sequences

To start the EP transfers according to a defined scenario, the coordinator is instructed to initiate the sequence as defined in a configuration file. Fig. 13 shows measurements for a scenario, where adjacent EP transfers are chained such that a continuous power flow is achieved. The upper plot shows measurements captured on the signal processing platform, where the signals sampled with $f_{\mathrm{s}} = 50\,\mathrm{kHz}$ are averaged over a $4\,\mathrm{ms}$ window. The lower plot shows measurements of the same event obtained with an oscilloscope. At $t = 5\,\mathrm{s}$, the first EP transfer between devices 1 and 2 with $i_{\mathrm{EP}} = 5\,\mathrm{A}$ enters its downward ramping phase that lasts $t_{\mathrm{r}} = 2\,\mathrm{s}$. At the same time, another transfer with the same ramping slope and stationary power is initiated between devices 1 and 3, such that device 1 continues to output the same power. At $t = 6\,\mathrm{s}$, this transfer is again replaced and the simultaneous ramping results in a linear transition into the lower stationary power of this transfer. The total energy transferred in this sequence is $W_{\mathrm{seq}} = \int_{t_0}^{t_0+t_{seq}} \sum_i p_{EP,i}(\tau)d\tau = 27\,\mathrm{kJ} = 7.5\,\mathrm{W\,h}$.

Measurements for a second scenario are shown in Fig. 14. In this case, the focus is on transferring multiple parallel energy packets from one device. The ramping phases are set to $t_{\mathrm{r}} = 1\,\mathrm{ms}$, resulting in almost rectangular power curves. At $t = 2\,\mathrm{s}$, devices 1 and 2 start an EP transfer with a duration of $t_{\mathrm{EP}} = 10\,\mathrm{s}$ and a stationary current of $i_{\mathrm{EP}} = 2.5\,\mathrm{A}$. At $t = 6\,\mathrm{s}$, device 1 increases its power by initiating a second transfer with a current of $i_{\mathrm{EP}} = 5\,\mathrm{A}$. At $t = 8\,\mathrm{s}$, the power supplied by device 1 is yet again increased to a total of $i_{\mathrm{DC},1} = 10\,\mathrm{A}$ with a third transfer to device 3 with a current of $i_{\mathrm{EP}} = 2.5\,\mathrm{A}$. The energy transferred by this sequence is $W_{\mathrm{seq}} = 55\,\mathrm{kJ} = 15.3\,\mathrm{W\,h}$. In this measurement, the impact of communication delays is visible due to short ramping phases. Both at $t = 3\,\mathrm{s}$ and $t = 9\,\mathrm{s}$, the voltage controller compensates for the mismatch in the currents supplied and drawn by devices 1 and 2. In the presented measurements, the DC bus voltage is constant at $v_{\mathrm{DC}} = 600\,\mathrm{V}$ for all EP devices. If this voltage instead varies, the controlled currents $i_{\mathrm{DC,x}}$ will also be adjusted during the transfer to maintain the negotiated power flow.

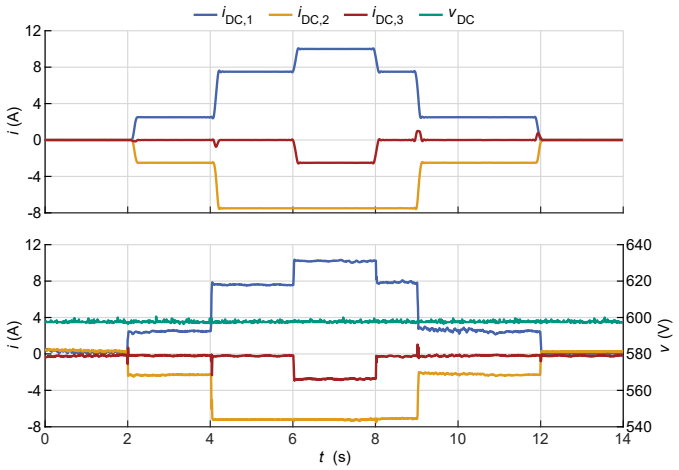


Fig. 14: Measurements for parallel EP transfers

## VI. Conclusion

This paper explores the concept of coordinated energy packet transfers in the Energy Packet Grid and its potential for shaping power flows and improving power flow control in future grids with distributed energy resources and flexible demand. The coordinated dispatch enables continuous power levels over different transfers and the approximation of continuous power flows. A central coordinator and necessary interfaces are implemented in this work and the approach is verified through experimental measurements, which demonstrate the desired power flow patterns. In this way, the paper serves as a foundation for further exploration and development in the field based on the presented architecture and concepts.

## References


[1] R. Gupta, A. Pena-Bello, K. N. Streicher, C. Roduner, Y. Farhat, D. Thöni, M. K. Patel, and D. Parra, "Spatial analysis of distribution grid capacity and costs to enable massive deployment of PV, electric mobility and electric heating," *Applied Energy*, vol. 287, p. 116504, Apr. 2021.

[2] H. K. Çakmak and V. Hagenmeyer, "Using Open Data for Modeling and Simulation of the All Electrical Society in eASiMOV," in *2022 Open Source Modelling and Simulation of Energy Systems (OSMSES)*, Apr. 2022, pp. 1–6.

[3] P. Palensky and D. Dietrich, "Demand Side Management: Demand Response, Intelligent Energy Systems, and Smart Loads," *IEEE Transactions on Industrial Informatics*, vol. 7, no. 3, pp. 381–388, Aug. 2011.

[4] S. Kampezidou, O. Vasios, and S. Meliopoulos, "Multi-Microgrid Architecture: Optimal Operation and Control," in *2018 North American Power Symposium (NAPS)*. Fargo, ND: IEEE, Sep. 2018, pp. 1–5.

[5] G. Kariniotakis, L. Martini, C. Caerts, H. Brunner, and N. Retiere, "Challenges, innovative architectures and control strategies for future networks: The Web-of-Cells, fractal grids and other concepts," *CIRED - Open Access Proceedings Journal*, vol. 2017, pp. 2149–2152, Oct. 2017.

[6] P. H. J. Nardelli, H. Alves, A. Pinomaa, S. Wahid, M. D. C. Tomé, A. Kosonen, F. Kühnlenz, A. Pouttu, and D. Carrillo, "Energy Internet via Packetized Management: Enabling Technologies and Deployment Challenges," *IEEE Acc.*, vol. 7, pp. 16 909–16 924, 2019.

[7] K. A. Corzine, "Energy packets enabling the energy internet," in *2014 Clemson University Power Systems Conf.*, Mar. 2014, pp. 1–5.

[8] R. Takahashi, K. Tashiro, and T. Hikihara, "Router for Power Packet Distribution Network: Design and Experimental Verification," *IEEE Transactions on Smart Grid*, vol. 6, no. 2, pp. 618–626, Mar. 2015.

[9] D. Boroyevich, I. Cvetkovic, R. Burgos, and D. Dong, "Intergrid: A Future Electronic Energy Network?" *IEEE Journal of Emerging and Selected Topics in Power Electronics*, vol. 1, no. 3, pp. 127–138, Sep. 2013.

[10] J. Ma, L. Song, and Y. Li, "Optimal Power Dispatching for Local Area Packetized Power Network," *IEEE Transactions on Smart Grid*, vol. 9, no. 5, pp. 4765–4776, Sep. 2018.

[11] R. Rojas-Cessa, C. Wong, Z. Jiang, H. Shah, H. Grebel, and A. Mohamed, "An Energy Packet Switch for Digital Power Grids," in *2018 IEEE International Conference on Internet of Things (iThings) and IEEE Green Computing and Communications (GreenCom) and IEEE Cyber, Physical and Social Computing (CPSCom) and IEEE Smart Data (SmartData)*, Jul. 2018, pp. 146–153.

[12] I. Kouveliotis-Lysikatos, N. Hatziargyriou, Y. Liu, and F. Wu, "Towards an Internet-Like Power Grid," *Journal of Modern Power Systems and Clean Energy*, pp. 1–11, 2020.

[13] A. Khurram, M. Amini, L. A. D. Espinosa, P. D. H. Hines, and M. R. Almassalkhi, "Real-Time Grid and DER Co-Simulation Platform for Testing Large-Scale DER Coordination Schemes," *IEEE Transactions on Smart Grid*, vol. 13, no. 6, pp. 4367–4378, Nov. 2022.

[14] L. A. D. Espinosa, A. Khurram, and M. Almassalkhi, "Reference-Tracking Control Policies for Packetized Coordination of Heterogeneous DER Populations," *IEEE Transactions on Control Systems Technology*, vol. 29, no. 6, pp. 2427–2443, Nov. 2021.

[15] P. Rezaei, J. Frolik, and P. D. H. Hines, "Packetized Plug-In Electric Vehicle Charge Management," *IEEE Transactions on Smart Grid*, vol. 5, no. 2, pp. 642–650, Mar. 2014.

[16] K. Schneider, F. Wiegel, D. Schulz, V. Hagenmeyer, M. Hiller, R. Bless, and M. Zitterbart, "Designing the Interplay of Energy Plane and Communication Plane in the Energy Packet Grid," in *IEEE Conf. on Local Computer Networks (LCN)*, Oct. 2021, pp. 331–334.

[17] D. Schulz, K. Schneider, M. Weßbecher, V. Hagenmeyer, M. Zitterbart, and M. Hiller, "Hardware Realization of Participants in an Energy Packet-based Power Grid," in *Int. Symp. on Power Electronics for Dist. Gen. Systems (PEDG)*, Jun. 2022, pp. 1–6.

[18] K. Schneider, D. Schulz, M. Weßbecher, V. Hagenmeyer, M. Hiller, and M. Zitterbart, "Modes of energy packets in the energy packet grid," in *2023 8th IEEE Workshop on the Electronic Grid (eGRID)*, in submission.

[19] G. Zieglmaier, F. Sommer, T. Merz, and M. Hiller, "Highly Dynamic Voltage Control of a Dual Active Bridge over the Full Voltage Range by Operating Point Dependent Manipulated Variable Limitation," in *PCIM Europe 2023; International Exhibition and Conference for Power Electronics, Intelligent Motion, Renewable Energy and Energy Management*, May 2023, pp. 1–10.